===== **DIELECTRICS** =====

Electronic Structure, Optical Properties, and Pressure Behavior of the CdB$_4$O$_7$ and HgB$_4$O$_7$ Compounds

A. S. Shinkorenko[a], *, V. I. Zinenko[a], and M. S. Pavlovskii[a]

[a] *Kirensky Institute of Physics, Federal Research Center "Krasnoyarsk Scientific Center,"*
Russian Academy of Sciences, Siberian Branch, Krasnoyarsk, 660036 Russia
e-mail: shas@iph.krasn.ru

Abstract—Ab initio calculations of the structural, electronic, and optical properties of the HgB$_4$O$_7$ and CdB$_4$O$_7$ tetraborate compounds in three structural modifications with the *Pbca*, *Cmcm*, and *Pmn*2$_1$ symmetry have been performed in the framework of the density functional theory using the VASP package. The calculations of the electronic band structure showed that these compounds in all the investigated modifications are dielectrics with a band gap of 2−4 eV. The calculation of the structural properties of the tetraborates under pressure showed that the phase transition between the *Pbca* and *Pmn*2$_1$ structures in cadmium and mercury tetraborates occurs under pressures of 4.8 and 4.7 GPa, respectively.

1. INTRODUCTION

The borate compounds with the chemical formula M^{+2}B$_4$O$_7$ have some interesting features, including luminescence and nonlinear optical and electrical properties [1]. These properties can be important for application. In addition, they are interesting from the crystallochemical point of view. These compounds exist in several basic structural forms containing BO$_3$ (triangles) and/or BO$_4$ (tetrahedra). The experiments showed [2−10] that, depending on the M^{+2} ion radius and external conditions, the M^{+2}B$_4$O$_7$ compounds can exist, with some exceptions, in two of the three basic structural types [11].

The first structural type belongs to the space symmetry group *Pbca*. The structure of this type is based on the boron−oxygen frame consisting of vortex-sharing BO$_4$ tetrahedra and BO$_3$ triangles (in the one-to-one ratio). Cavities of such a frame contain M^{+2} atoms. This structural type is implemented, as a rule, in the compounds where the ionic radius of a metal lies between 0.9−1 Å. In the compounds with a metal ionic radius of smaller than 1 Å at high temperatures and pressures, the second structural type with the symmetry group *Cmcm* is implemented. In contrast to the structure with the sp. gr. *Pbca*, it only contains boron-oxygen tetrahedra BO$_4$. Finally, the third structural type has the polar group *Pmn*2$_1$, consists also of only BO$_4$ tetrahedra, and is implemented under normal pressure in the compounds with the metal ion radius larger than 1.3 Å. In the compounds with a metal ion radius between 1.1 Å < 1.3 Å, this structural type is implemented under high pressures. Cadmium and mercury ions have an ionic radius of ~1.15 Å; it can be expected that all the three structural types can be implemented in tetraborates with these ions.

For mercury tetraborate, both the normal [12] and high-pressure phase [9] were established. For the cadmium tetraborate compound, only the normal-pressure phase was experimentally found [13]. Winkler et al. [14] examined the phase diagram of CdB$_4$O$_7$ under hydrostatic pressure using ab initio calculations. According to the calculated data, under a pressure of 5 GPa cadmium tetraborate undergoes the phase transition from *Pbca* to *Cmcm*. Literature data on the electronic and optical properties of these compounds are lacking.

Here, we report the results of ab initio calculations of the structural, electronic, and optical properties of cadmium and mercury tetraborates in the phases with the *Pbca*, *Cmcm*, and *Pmn*2$_1$ structures and their phase diagram under pressure.

2. CALCULATION TECHNIQUE

The calculations were performed by the projector augmented wave (PAW) method [15, 16] in the framework of the density functional theory (DFT) implemented in the Vienna ab initio simulation package (VASP) [17, 18]. The generalized gradient approximation (GGA) with the Perdew−Burke−Ernzerhof parametrization was used [19]. The selected electron configurations of the atomic potentials were 4d^{10}5s^2 for Cd, 5d^{10}6s^2 for Hg, 2$s^2$2p^1 for B, and 2$s^2$2p^4 for O. The
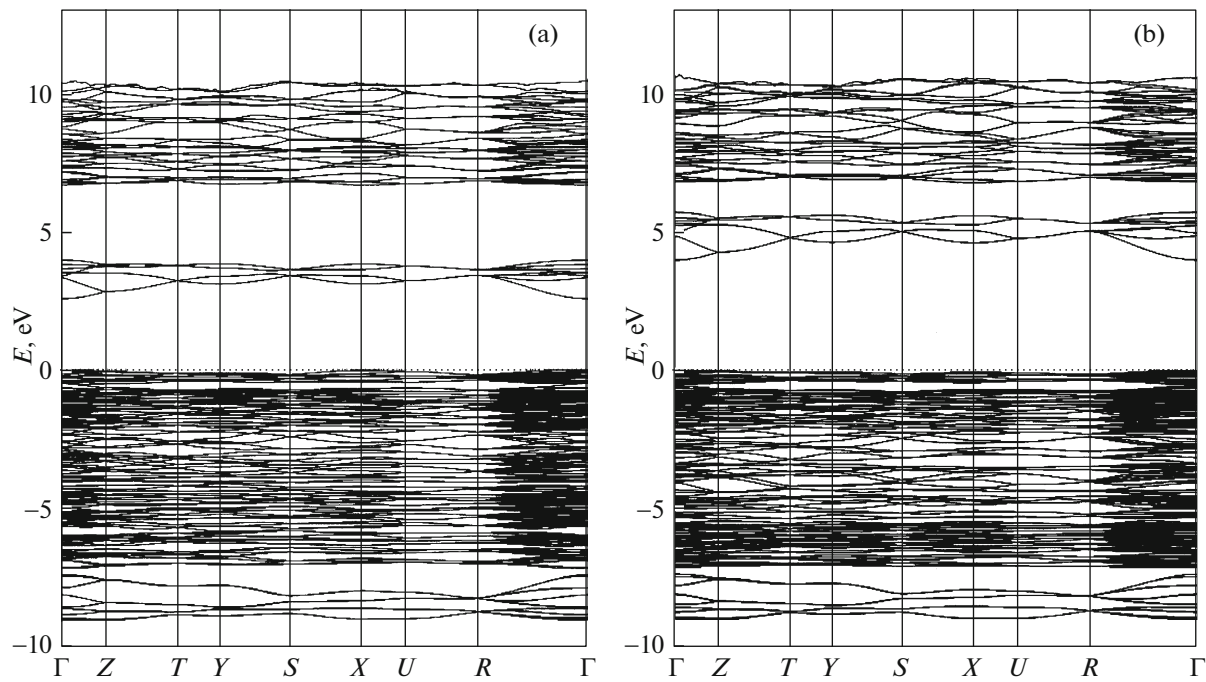
Fig. 1. Calculated electronic band structure of (a) the HgB_4O_7 and (b) CdB_4O_7 compounds in the *Pbca* structure.

number of plane waves was limited to an energy of 600 eV. The sizes of the k-point grid based on the Monkhorst–Pack scheme [20] were $4 \times 5 \times 3$ for the *Pbca* structure, $4 \times 6 \times 8$ for the *Cmcm* structure, and $4 \times 9 \times 9$ for the $Pmn2_1$ structure. In the density-of-states (DOS) calculation, the k-point grid was doubled in each direction. The structural geometry was optimized until the residual forces became lower than 1 meV/Å.

The electronic structure and optical properties were calculated for the relaxed lattice parameters and coordinates.

3. ELECTRONIC STRUCTURE

Tables 1–3 give the calculated cell parameters and relative atomic coordinates for the three structural modifications of the CdB_4O_7 and HgB_4O_7 compounds together with the available experimental literature data. It can be seen that both the cell parameters and atomic coordinates are in good agreement with the experimental data.

The calculated electronic band structure of the CdB_4O_7 and HgB_4O_7 compounds in the structure with sp. gr. *Pbca* is shown in Fig. 1. There are no qualitative differences in the electronic structure of these compounds. The total (TDOS) and partial (PDOS) densities of states for the investigated compounds in the three structures are presented in Fig. 2. All the TDOS and PDOS are normalized to the formula unit. The band gaps ΔE of different structures of the investigated compounds are given in Table. 4.

The calculated electron TDOS and PDOS for the different structural types of the CdB_4O_7 and HgB_4O_7 crystals are not qualitatively different. It can be seen that the valence band structures for all the modifications of the compounds under study are almost identical and consist of the d states of M^{2+} atoms (the middle of the band and the high peak), s and p states of B atoms (the center and bottom of the band), and p states of O atoms (the center and upper part of the band).

The most significant differences are observed in the conduction band for all the structural types. In all the investigated cases, the narrow lower part of the conduction band is separated from the main part (this energy interval ΔE_1 is given in Table 4). This lower part of the conduction band consists of the s states of electrons of M^{2+} atoms and p states of electrons of O atoms. Depending on the structure and composition, the bottom of the conduction band changes its position relative to the upper part of the valence band, which, in turn, changes the band gap. The widest band gap is observed in the structure with the symmetry group *Cmcm* and the narrowest band gap corresponds to the $Pmn2_1$ structure. The upper part of the conduction band for all the structural types and compounds consists of the p states of electrons of each atom.

In mercury tetraborate of all the structural types, the band gap is narrower than in cadmium tetraborate, since the excited s states of electrons of Hg ions are located at a lower energy level than the excited s states of electrons of Cd ions [21]. The upper part of the con-

Table 1. Calculated and experimental (in parenthesis) atomic coordinates and lattice parameters of the CdB_4O_7 [13] and HgB_4O_7 [12] compounds with the *Pbca* structure ($Z = 8$)

Pbca	*a*	*b*	*c*
CdB_4O_7	8.41 (8.21) Å	8.90 (8.70) Å	14.34 (14.18) Å
HgB_4O_7	8.548 (8.399) Å	8.955 (8.806) Å	14.371 (14.137) Å
M^{Cd}	0.1262 (0.1210)	0.1105 (0.1105)	0.6138 (0.6125)
M^{Hg}	0.1393 (0.1394)	0.1157 (0.1122)	0.1174 (0.1169)
B_1^{Cd}	0.4453 (0.4473)	0.2830 (0.2864)	0.5647 (0.5679)
B_1^{Hg}	0.4516 (0.4542)	0.2876 (0.2810)	0.0623 (0.0616)
B_2^{Cd}	0.0156 (0.0140)	0.3218 (0.3385)	0.7658 (0.7654)
B_2^{Hg}	0.5076 (0.5109)	0.3343 (0.3294)	0.2336 (0.2348)
B_3^{Cd}	0.0091 (0.0061)	0.0684 (0.0640)	0.8376 (0.8376)
B_3^{Hg}	0.5188 (0.5165)	0.0699 (0.0632)	0.1618 (0.1609)
B_4^{Cd}	0.2048 (0.2019)	0.1476 (0.1374)	0.9549 (0.9575)
B_4^{Hg}	0.7152 (0.7176)	0.1557 (0.1487)	0.0490 (0.0489)
O_1^{Cd}	0.0479 (0.0543)	0.4225 (0.4103)	0.6920 (0.6875)
O_1^{Hg}	0.0337 (0.0426)	0.4246 (0.4173)	0.1924 (0.1895)
O_2^{Cd}	0.3890 (0.3853)	0.1387 (0.1325)	0.5994 (0.5980)
O_2^{Hg}	0.4030 (0.4003)	0.1346 (0.1332)	0.0951 (0.0933)
O_3^{Cd}	0.3489 (0.3544)	0.3691 (0.3759)	0.4996 (0.5021)
O_3^{Hg}	0.3574 (0.3627)	0.3584 (0.3646)	−0.0059 (0.0064)
O_4^{Cd}	0.4693 (0.4733)	0.3856 (0.3837)	0.6477 (0.6469)
O_4^{Hg}	0.4611 (0.4651)	0.3845 (0.3834)	0.1467 (0.1474)
O_5^{Cd}	0.0322 (0.0335)	0.1773 (0.1642)	0.7567 (0.7545)
O_5^{Hg}	0.5300 (0.5288)	0.1810 (0.1730)	0.2440 (0.2448)
O_6^{Cd}	0.1016 (0.1094)	0.2611 (0.2561)	0.9831 (0.9799)
O_6^{Hg}	0.6120 (0.6153)	0.2679 (0.2650)	0.0210 (0.0208)
O_7^{Cd}	0.1634 (0.1595)	0.0546 (0.0428)	0.8853 (0.8841)
O_7^{Hg}	0.6725 (0.6733)	0.0526 (0.0617)	0.1189 (0.1180)

duction band in both compounds is located at approximately the same energy level.

4. OPTICAL PROPERTIES

For all the CdB_4O_7 and HgB_4O_7 structural types, we calculated the dielectric function [22] and absorption coefficient α as a function of frequency [23]

$$\alpha(\omega) = \frac{2\omega}{c} \sqrt{\frac{|\varepsilon(\omega)| - \varepsilon'(\omega)}{2}},$$

where $\varepsilon(\omega)$ is the complex dielectric function and $\varepsilon'(\omega)$ is the real part of the dielectric function. The calculated dependences of the absorption coefficient are presented in Fig. 3. Since we observed no significant anisotropy of the optical properties, the average values of the absorption coefficient are shown. Using these dependences, we determined the material absorption edges *Pbca* ~ 300 nm, *Cmcm* ~ 250 nm, and *Pmn*2_1 ~ 350 nm for the three CdB_4O_7 crystal structures and *Pbca* ~ 440 nm, *Cmcm* ~ 370 nm, and *Pmn*2_1 ~ 600 nm for the HgB_4O_7 crystal. The obtained absorption edges

Table 2. Calculated atomic coordinates and lattice parameters of the CdB_4O_7 and HgB_4O_7 compounds with the *Cmcm* structure ($Z = 4$)

Cmcm	a	b	c
CdB_4O_7	11.062 Å	6.838 Å	5.325 Å
HgB_4O_7	11.118 Å	6.896 Å	5.383 Å
M^{Cd}	0.0000	0.2163	0.2500
M^{Hg}	0.0000	0.2162	0.2500
B_1^{Cd}	0.7105	0.0000	0.0000
B_1^{Hg}	0.7123	0.0000	0.0000
B_2^{Cd}	0.6213	0.2886	0.2500
B_2^{Hg}	0.6222	0.2861	0.2500
O_1^{Cd}	0.0000	0.8851	0.2500
O_1^{Hg}	0.0000	0.8776	0.2500
O_2^{Cd}	0.2872	0.4698	0.2500
O_2^{Hg}	0.2882	0.4674	0.2500
O_3^{Cd}	0.1380	0.3267	−0.0285
O_3^{Hg}	0.1407	0.3285	−0.0317

correspond to the peculiarities of the above-described calculated band structures.

5. ELASTIC PROPERTIES AND BEHAVIOR UNDER HYDROSTATIC PRESSURE

It was experimentally established that the hydrostatic pressure affects the formation of BO_4 boron-oxygen tetrahedra in the structures during the growth of crystals of divalent metal teraborates. In the compounds with a small divalent ion radius, the structures with sp. gr. *Pbca* and *Cmcm* usually compete. For example, the ZnB_4O_7 compound under normal pressure crystallizes in the sp. gr. *Pbca* and, under the high pressure, in the sp. gr. *Cmcm* [8]. In the compounds with the large ionic radius, the structures with the sp. gr. *Pbca* and $Pmn2_1$ compete. For example, SnB_4O_7 under high pressure crystallizes in the sp. gr. $Pmn2_1$. The SnB_4O_7 phase structure under normal pressure was not established [9]. The boundary ionic radius, at which all the three investigated structural types can compete, is approximately ~1.15 Å. Such an ionic radius is typical of Cd atoms (R_{Cd} = 1.15 Å) and Hg atoms (R_{Hg} = 1.14 Å). The energy favor of the phases with the sp. gr. $Pmn2_1$ and *Cmcm* (where, as was mentioned above, there are only the BO_4 tetrahedra) under high pressures as compared with the phase with the sp. gr. *Pbca* (where the BO_4 tetrahedra and BO_3 triangles are contained in equal proportion) is apparently

Table 3. Calculated and experimental [11] atomic coordinates and lattice parameters of the CdB_4O_7 and HgB_4O_7 with the $Pmn2_1$ structure ($Z = 2$)

| $Pmn2_1$	a	b	c
CdB_4O_7	10.769 Å	4.420 Å	4.226 Å
HgB_4O_7	10.825 (10.656) Å	4.445 (4.381) Å	4.239 (4.187) Å
M^{Cd}	0.0000	0.1648	0.1033
M^{Hg}	0.0000 (0.0000)	0.1800 (0.1802)	0.1033 (0.1033)
B_1^{Cd}	0.8794	0.6721	0.6359
B_1^{Hg}	0.8794 (0.8796)	0.6768 (0.6738)	0.5869 (0.5900)
B_2^{Cd}	0.7510	0.8259	0.1596
B_2^{Hg}	0.7513 (0.7513)	0.8301 (0.8258)	0.0696 (0.0704)
O_1^{Cd}	0.7777	0.8644	0.8027
O_1^{Hg}	0.7791 (0.7762)	0.8700 (0.8637)	0.4197 (0.4272)
O_2^{Cd}	0.8600	0.3530	0.7127
O_2^{Hg}	0.8583 (0.8615)	0.3586 (0.3518)	0.5153 (0.5155)
O_3^{Cd}	0.8661	0.7316	0.2985
O_3^{Hg}	0.8653 (0.8667)	0.7361 (0.7275)	0.9235 (0.9322)
O_4^{Cd}	0.000	0.7716	0.7456
O_4^{Hg}	0.0000 (0.0000)	0.7701 (0.7770)	0.4787 (0.4809)

Table 4. Calculated band gaps ΔE and ΔE_1 of the CdB_4O_7 and HgB_4O_7 compounds with different structures

	CdB_4O_7			HgB_4O_7		
	Pbca	*Cmcm*	$Pmn2_1$	*Pbca*	*Cmcm*	$Pmn2_1$
ΔE, eV	3.9	4.6	3.1	2.57	3.0	1.9
ΔE_1, eV	1.0	0.9	2.9	2.7	2.2	4.1

Table 5. Calculated values of Cii [GPa] for compounds CdB_4O_7 and HgB_4O_7 in different structures

		C_{11}	C_{22}	C_{33}	C_{12}	C_{13}	C_{23}	C_{44}	C_{55}	C_{66}
CdB_4O_7	*Pbca*	87	85	89	17	34	39	20	32	50
	Cmcm	370	318	338	147	128	114	85	131	115
	$Pmn2_1$	261	272	334	30	30	28	64	90	78
HgB_4O_7	*Pbca*	93	91	66	16	24	38	15	30	47
	Cmcm	352	302	321	148	136	110	84	121	96
	$Pmn2_1$	267	279	335	42	40	42	38	93	56

related to the difference between the chemical bonds in these phases and, consequently, to the difference between the elastic properties. Table 5 gives the calcu-
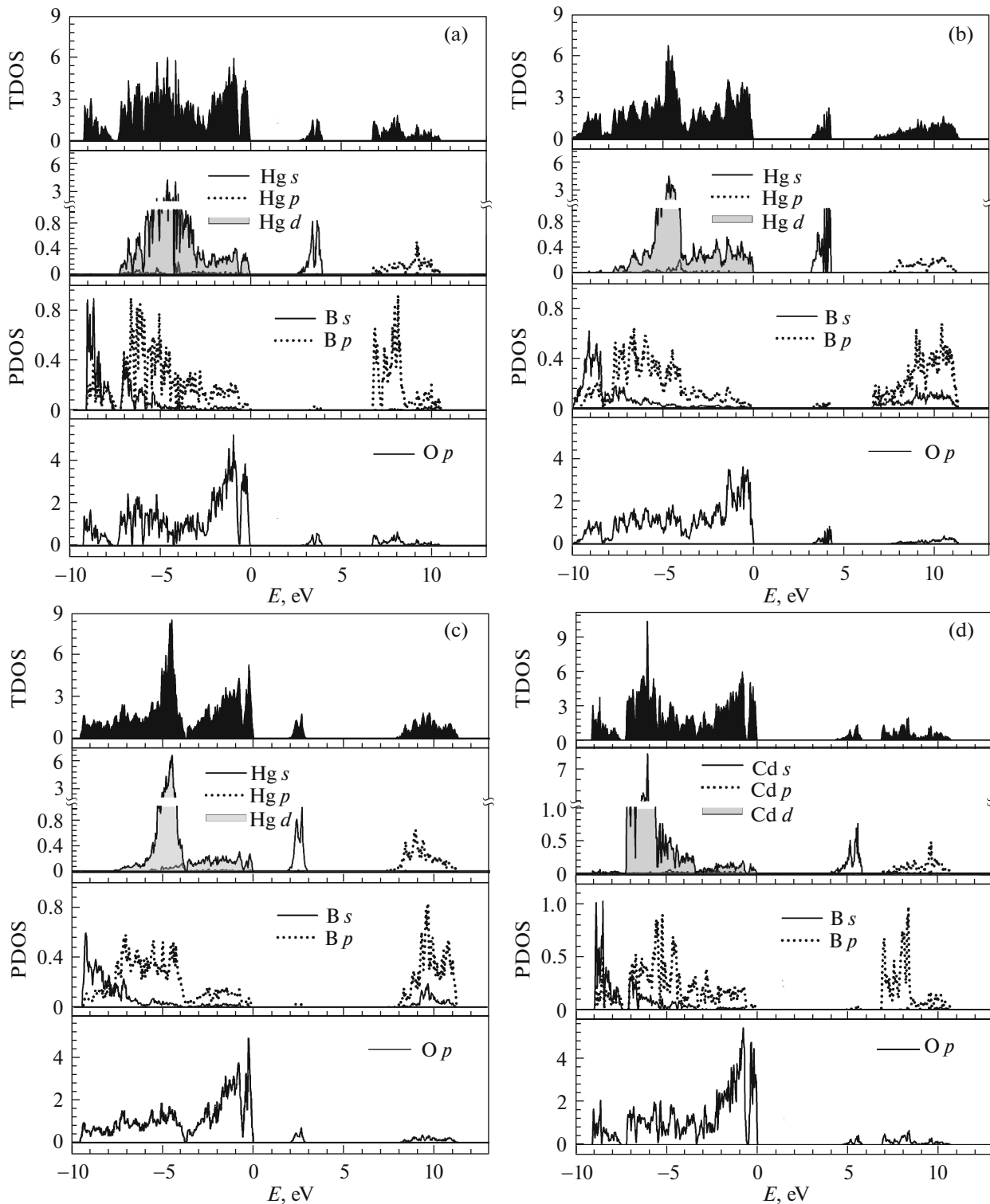
Fig. 2. Calculated TDOS and PDOS of the HgB_4O_7 (a, b, c) and CdB_4O_7 (d, e, f) compounds in the *Pbca*, *Cmcm*, and *Pmn*2_1 structures, respectively.

lated elastic constants for CdB_4O_7 and HgB_4O_7 in the phases with the sp. gr. *Pmn*2_1, *Cmcm*, and *Pbca*.

It can be seen from Table 5 that the elastic properties of the investigated compounds in the *Pmn*2_1 and *Cmcm* structures containing only the boron-oxygen tetrahedra are significantly different from the elastic properties of these compounds with the *Pbca* structure consisting of the boron-oxygen triangles and tetrahedra in equal proportion.
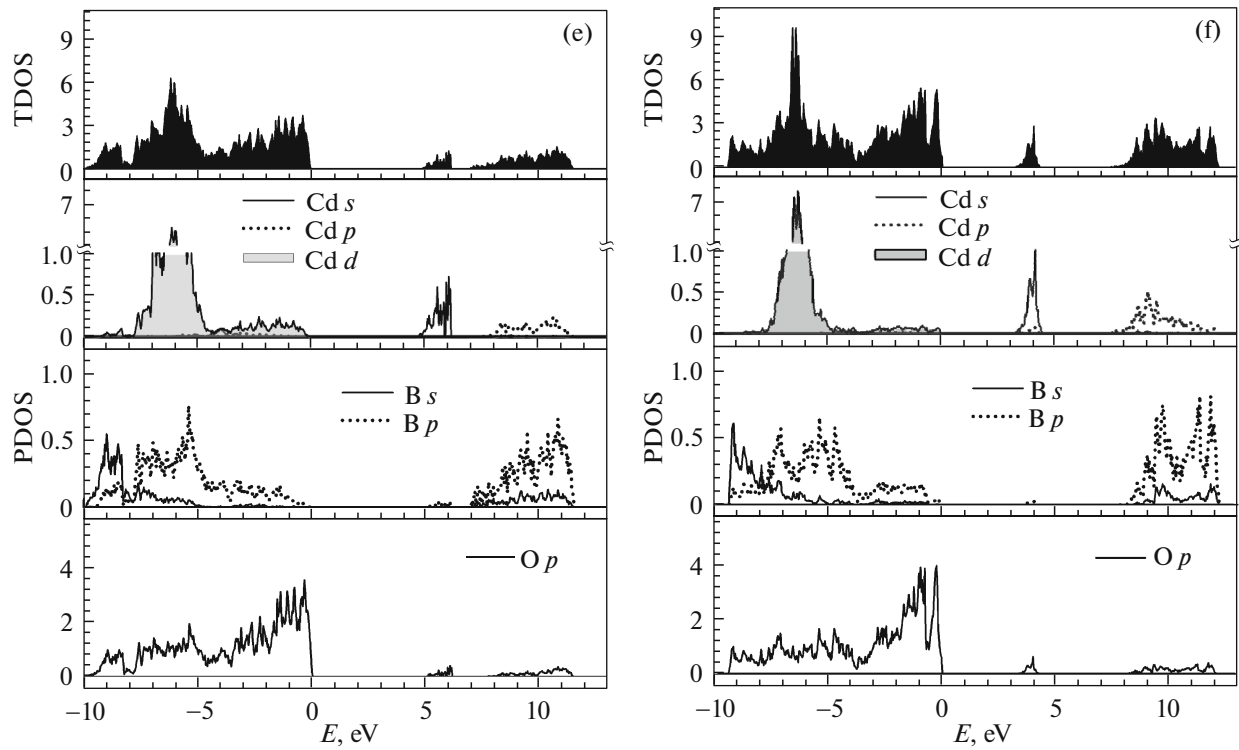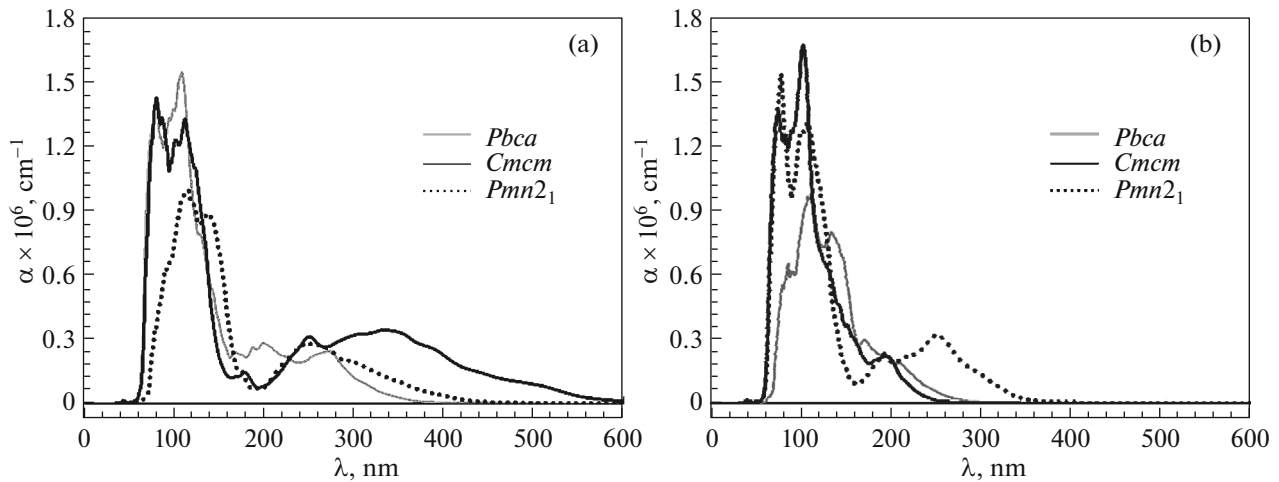
Fig. 2. (Contd.)

Fig. 3. Calculated wavelength dependence of absorption coefficient a for (a) the HgB_4O_7 and (b) CdB_4O_7 compounds with different structures.

To estimate the pressure of the phase transitions in the CdB_4O_7 and HgB_4O_7 crystals, the relaxation of the cell parameters and ion coordinates under certain hydrostatic pressures was performed for each of the $Pbca$, $Cmcm$, and $Pmn2_1$ phases. Under each pressure, the enthalpies $H = E + PV$ (where E is the total energy of the crystal, P is the pressure, and V is the cell volume) per one formula unit were compared. The results of the calculation are shown in Fig. 4. It can be seen

that the phase transition from $Pbca$ to $Pmn2_1$ in cadmium tetraborate occurs under a pressure of 4.8 GPa. The same phase transition in mercury tetraborate occurs under a pressure of 4.7 GPa. The obtained pressures of the phase transition in mercury tetraborate is qualitatively consistent with the experimental data reported in [9], where the HgB_4O_7 crystal in the $Pmn2_1$ phase was grown under a pressure of 7.5 GPa. In the presented calculations, the phase transition
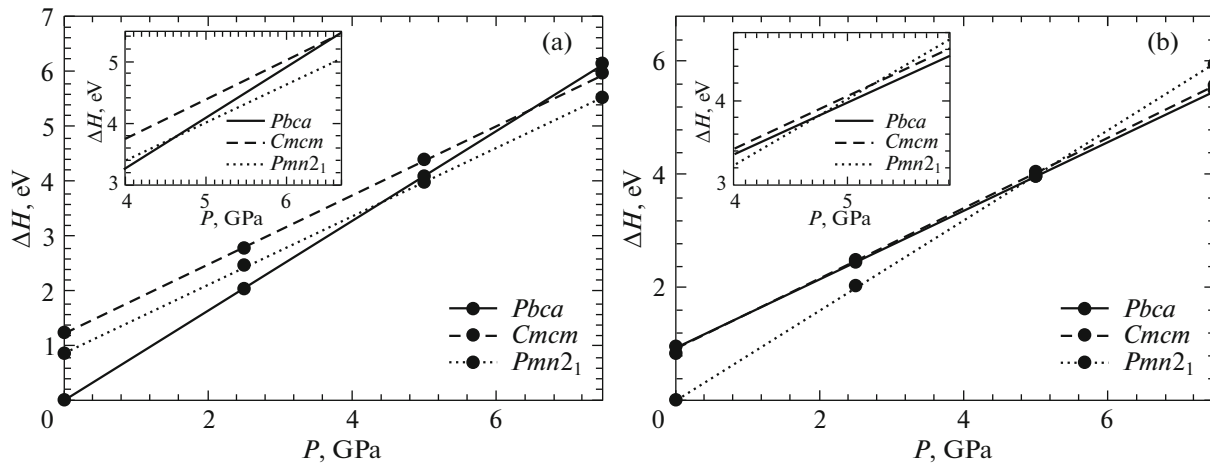
Fig. 4. Pressure dependence of the difference between the enthalpies of (a) the HgB_4O_7 and (b) CdB_4O_7 compounds with three structures. The reference point is energy.

from *Pbca* to *Cmcm* was not observed. It is worth noting that the difference between the energies of the *Cmcm* and *Pmn2_1* phases in the CdB_4O_7 compound is very low over the entire pressure range ($\Delta E_{tot} = 0.05$ eV per formula) used in the calculation.

6. CONCLUSIONS

In the framework of the density functional theory with the use of the VASP package, the structural, electronic, and optical properties of mercury and cadmium tetraborates were calculated for their three structural modifications with the *Pbca*, *Cmcm*, and *Pmn2_1* symmetry. The calculation showed that in both compounds with all the investigated structures, the energy gap between the valence and conduction bands is about 2—4 eV. The specific feature of the electronic structure of these compounds is that the lower part of the conduction band represents a narrow region from the *s* states of electrons of metal atoms and the *p* states of electrons of oxygen atoms, which is separated from the main part of the conduction band by several electronvolts.

The calculation showed that the elastic properties of the compounds under investigation in the *Pmn2_1* and *Cmcm* structures consisting of boron-oxygen tetrahedra significantly differ from the elastic properties of these compounds with the *Pbca* structure consisting of boron-oxygen triangles and tetrahedra in equal proportion. The properties of cadmium and mercury tetraborates in different phases under pressure were examined. The calculations of the CdB_4O_7 and HgB_4O_7 properties under pressure showed that the phase transition between the *Pbca* and *Pmn2_1* structures of cadmium and mercury tetraborate occurs under pressures of 4.7 and 4.8 GPa, respectively. It is established that the transition between the *Cmcm* and *Pmn2_1* structures does not occur in the pressure range

(up to 50 GPa) used in our calculation. However, the energies of the phases with the *Pbca* and *Pmn2_1* structures in CdB_4O_7 are similar ($\Delta E_{tot} = 0.05$ eV per formula) over the entire pressure range of interest.

REFERENCES

1. P. Becker, Adv. Mater. **10**, 979 (1998).

2. M. Martinez-Rippol, S. Martinez-Carrera, and S. Garcia-Blanco, Acta Crystallogr., B **27**, 672 (1971).

3. R. D. Shannon, Acta Crystallogr., A **32**, 751 (1976).

4. M. Prokic, Nucl. Instrum. Methods Phys. Res. **175**, 83 (1980).

5. J. Krogh-Moe, Acta Chem. Scand. **18**, 2055 (1964).

6. K. Machida, H. Hata, K. Okuno, G. Adachi, and J. Shiokawa, J. Inorg. Nucl. Chem. **41**, 1425 (1979).

7. H. Huppertz, Z. Naturforsch. **58b**, 257 (2003).

8. H. Huppertz and G. Heymann, Solid State Sci. **5**, 281 (2003).

9. J. S. Knyrim, F. M. Schappacher, R. Pottgen, J. S. auf der Günne, D. Johrendt, and H. Huppertz, Chem. Mater. **19**, 254 (2007).

10. H. Emmea, M. Weilb, and H. Huppertz, Z. Naturforsch. B **60**, 815 (2005).

11. J. S. Knyrim, S. Romer, W. Schnick, and H. Huppertz, Solid State Sci. **11**, 336 (2009).

12. M. Weil, Acta Crystallogr., E **59**, 40 (2003).

13. M. Ihara and J. Krogh-Moe, Acta Crystallogr. **20**, 132 (1966).

14. B. Winkler, A. G. Castellanos Guzman, L. Wiehl, L. Bayarjargal, and V. Milman, Solid State Sci. **14**, 1080 (2012).

15. G. Kresse and D. Joubert, Phys. Rev. B **59**, 1758 (1999).

16. P. E. Blochl, Phys. Rev. B **50**, 17953 (1994).

17. G. Kresse and J. Hafner, Phys. Rev. B **47**, 558 (1993).

18. G. Kresse and J. Furthmüller, Phys. Rev. B **54**, 11169 (1996).

19. J. P. Perdew, in *Electronic Structures of Solids' 91*, Ed. by P. Ziesche and H. Eschrig (Akademie, Berlin, 1991), p. 11.

20. H. J. Monkhorst and J. D. Pack, Phys. Rev. B **13**, 5188 (1976).

21. J. A. Mc Leod, R. J. Green, N. A. Skorikov, L. D. Finkelstein, M. Abu-Samak, E. Z. Kurmaev, and A. Moewes, Proc. SPIE **7940**, 79400R-1 (2011).

22. M. Gajdoš, K. Hummer, G. Kresse, J. Furthmüller, and F. Bechstedt, Phys. Rev. B **73**, 045112 (2006).

23. F. Han, *A Modern Course in The Quantum Theory of Solids* (World Scientific, Singapore, 2012).

Translated by E. Bondareva